The Sc-Zr (Scandium-Zirconium) System

By A. Palenzona and S. Cirafici
University of Genova, Italy

Equilibrium Diagram

The equilibrium phases of the Sc-Zr system are: (1) the liquid, L; (2) the hexagonal, low-temperature continuous solid solution, (αSc, αZr); and (3) the bcc high-temperature continuous solid solution, (βSc, βZr). The assessed Sc-Zr phase diagram (Fig. 1) is based largely on the work of [63Bea], but changes in the melting points and transformation temperatures of Sc and Zr were made to agree with the accepted values listed in [86Gsc] and [Massalski]. No information is available for the liquidus curve; for this reason, the liquidus line is dashed.

[62Bea] and [63Bea] investigated the Sc-Zr equilibrium phase diagram by means of differential thermal analysis (DTA) for the determination of transformation points; temperatures were measured with an optical pyrometer. The metals employed were crystal bar Zr and distilled Sc (the major impurities present are listed in Table 1). The alloys were prepared directly in an arc-melting furnace under inert atmosphere. During preparation, approximately ≈0.5 at.% was lost, which was attributed entirely to the loss of Sc by distillation. Before X-ray analysis, samples were annealed 15 h at 550 °C. The solidus curve was determined, but the liquidus curve was not. The maximum in the α ↔ β transformation temperature was determined by [63Bea] with DTA, with an estimated ±1 at.% uncertainty in the composition of the maximum.

[71Dou], reviewing the diagram of [63Bea], observed that the transformation temperatures in the whole system could have been increased by the high oxygen content in the starting Sc metal (see Table 1). [60Spe] studied the corrosion resistance of Zr with additions of Sc to water at 310 °C. They noted that small additions (0.05 to 0.25 at.%) of Sc lowered the corrosion resistance of Zr but did not exclude the possibility that higher Sc additions could, on the contrary, enhance the corrosion resistance; however, their studies were inconclusive because of the high cost of Sc. All these results were reviewed and discussed in [71Dou], [76Kub], [Shunk], and [Moffatt].

Table 1 Impurity Analyses of Sc and Zr

Impurity	Contents, ppm(a) Sc	Zr
Fe	400	27
C	290	33
Al	100	25
Ti	20	8
N_2	100	10
Mg	25	25
Si	50	...
Cu	100	...
Ni	75	...
Ca	50	...
Cr	75	...
O_2	1100	...
Ta	250	...
F_2	475	...

From [63Bea].
(a) Not specified if wt. or at. ppm.

Metastable Phases

[74Wan] and [76Wan] studied the metastable solubility limits of primary cph solid solutions in RE-Zr systems. The alloys (2 g each) were prepared in a conventional arc furnace under an argon atmosphere. The rapid quenching of the alloys was performed in a purified argon atmosphere using a shock tube splat cooling apparatus. [74Wan] observed that the weight loss after the arc melting was less than 0.25 at.%, and therefore they assumed that the resulting solid solution phases retained the initial compositions. The solubility limits of the metastable solid solution were determined by an X-ray method. The lattice parameters were affected by an estimated systematic error of ±0.0005 nm. A complete series of solutions was found in the Sc-Zr system.

Crystal Structures and Lattice Parameters

Sc and Zr have the same cph, low-temperature (α) form and bcc, high-temperature (β) form, and the Sc-Zr system consists of continuous solid solutions at all temperatures. Crystal structures and lattice parameters are given in Table 2.

Table 2 Sc-Zr Crystal Structure and Lattice Parameter Data at 25 °C

Phase	Composition, at.% Zr	Pearson symbol	Space group	Strukturbericht designation	Prototype	Lattice parameters, nm a	c	Comment	Reference
(αSc,αZr)	0 to 100	*hP*2	$P6_3/mmc$	*A*3	Mg	0.33088	0.52680	Pure αSc	[86Gsc]
						0.32316	0.51475	Pure αZr	[Massalski]
(βSc,βZr)	0 to 100	*cI*2	$Im\bar{3}m$	*A*2	W	0.373	...	Pure βSc(a)	[86Gsc]
						0.36090	...	Pure βZr(b)	[Massalski]

(a) Estimated at 1312 °C. (b) At >863 °C.

[63Bea] determined lattice parameters for different compositions. Their X-ray data confirmed the complete solid solubility in this system at room temperature. These values are compiled in Table 3. The variation of the cph lattice parameters are also shown in Fig. 2. In contrast to other RE-Zr systems, the *a* and *c* parameters show, respectively, a positive and negative deviation from Vegard's law [75Gsc].

Thermodynamics

[84Lop] calculated the Gibbs energies of formation of substitutional solid solutions at 1000 K for systems like Sc-Zr. The calculations indicated that in the Sc-Zr system, the Gibbs energies of alloy formation are only slightly less than zero over the whole concentration range at 1000 K.

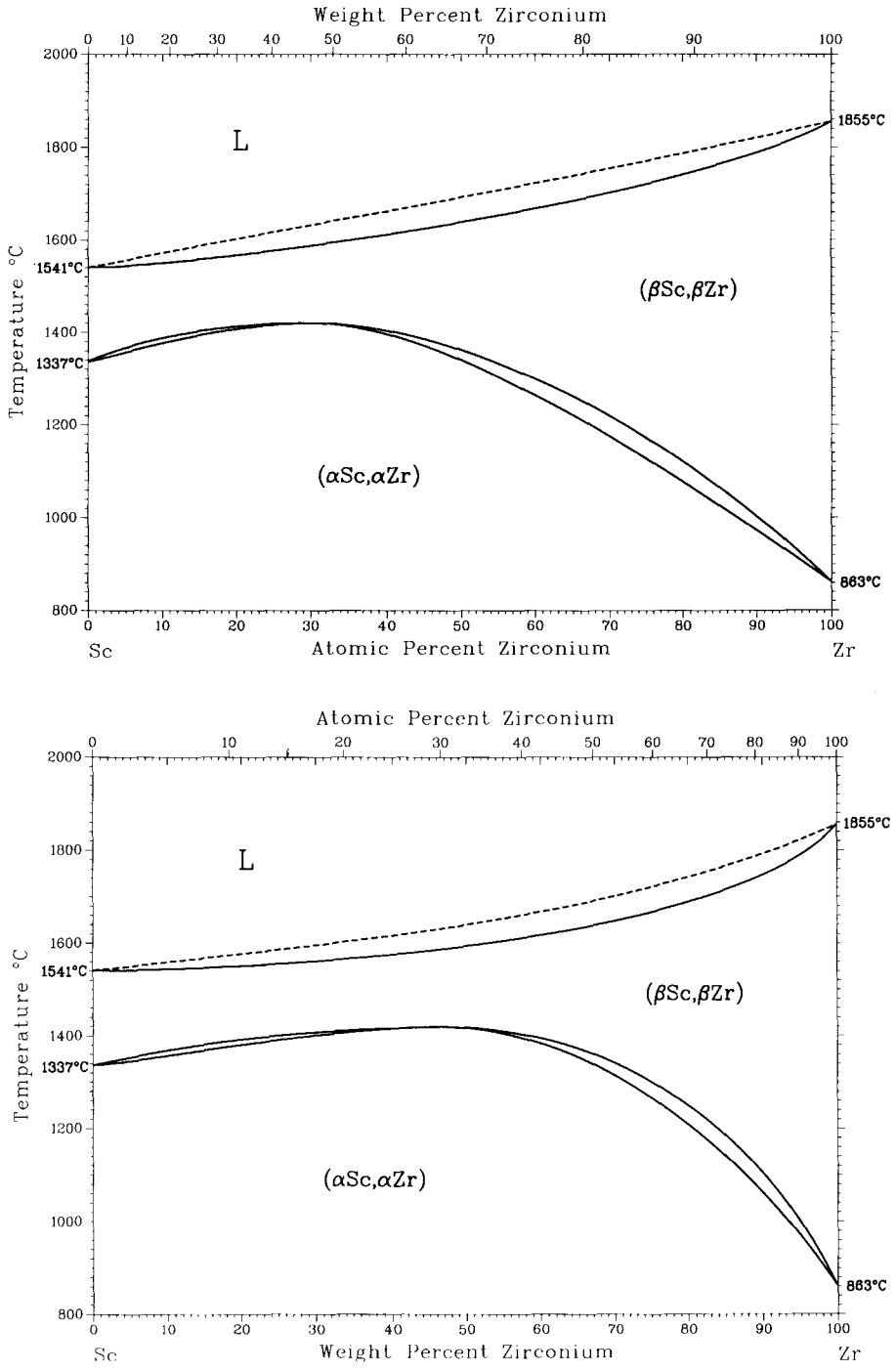

Fig. 1 Assessed Sc-Zr phase diagram.

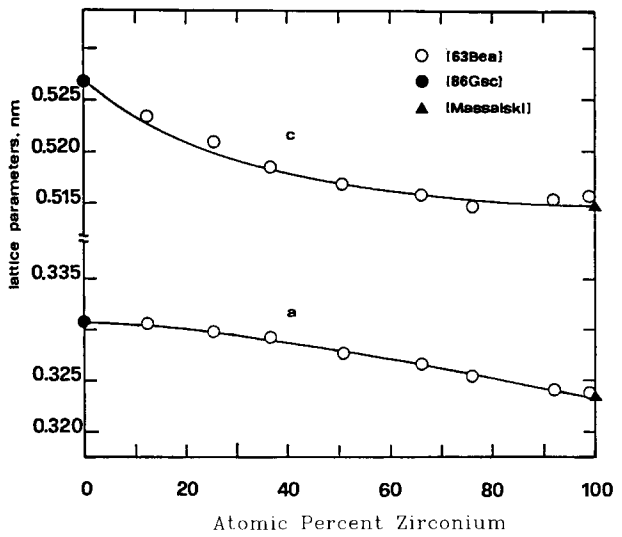

Fig. 2 Lattice parameters of (αSc,αZr) solid solution alloys.

Measurements of specific heat and Debye temperature were made at low temperature by [66Jen], [68Bet], and [80Tsa]; the independently determined values as reported in Table 4 show fairly good agreement. The γ for these alloys, after a correction for the phonon enhancement, correlates fairly well with the electronic density of states of pure Zr.

[78Ved] carried out resistivity and emf measurements on Sc-Zr alloys and found a regular behavior with composition, following the equation:

$$\rho \approx c\ (1-c)$$

where ρ is the resistivity in μΩ·cm and c is the composition in at.%.

Cited References

60Spe: F.H. Spedding and A.H. Daane, "Corrosion Resistance of Low-Scandium Zirconium Alloys," USAEC Rep. IS-192, 30-31 (1960). (Equi Diagram; Experimental)

62Bea: B.J. Beaudry and A.H. Daane, "The Scandium-Zirconium System," USAEC Rep. IS-596, 14 (1962). (Equi Diagram; Experimental)

***63Bea:** B.J. Beaudry and A.H. Daane, "The Scandium Yttrium and Scandium-Zirconium System," *Trans. Metall. Soc. AIME, 227,* 865-868 (1963). (Equi Diagram, Crys Structure; Experimental; #)

66Jen: M.A. Jensen and J.P. Maita, "Superconductivity and Electronic Specific Heat in the Scandium-Zirconium System," *Phys. Rev., 149,* 409-414 (1966). (Thermo; Experimental)

68Bet: J.O. Betterton, Jr. and J.O. Scarbrough, "Low-Temperature Specific Heats of Zr-Ti, Zr-Hf and Zr-Sc Alloys," *Phys. Rev., 168,* 715-725 (1968). (Equi Diagram, Thermo; Experimental)

71Dou: D.L. Douglass, "The Metallurgy of Zirconium," At. Energy Rev., Suppl., IAEA, Vienna (1971). (Equi Diagram; Review)

Table 3 Lattice Parameters of (αSc,αZr) Alloys

Composition, at.% Zr	Lattice parameters, nm *a*	*c*
12.3	0.3306	0.5234
25.5	0.3297	0.5211
36.7	0.3285	0.5185
50.7	0.3275	0.5168
66.0	0.3266	0.5157
76.1	0.3254	0.5147
92.1	0.3241	0.5155
99.0	0.3239	0.5158
99.8	0.3238	0.5157

From [63Bea].

Table 4 Electronic Specific Heat Coefficients (γ) and Debye Temperatures (θ_D) for (Sc,Zr) Alloys

Composition, at.% Zr	γ, mJ/mol·K²	θ_D, K	Reference
0.25	10.605	353.9	[80Tsa]
0.50	11.003	368.7	[80Tsa]
1.0	10.935	367.2	[80Tsa]
2.0	10.564	364.9	[80Tsa]
3.5	10.411	365.1	[80Tsa]
5.0	10.134	364.0	[80Tsa]
7.5	9.704	363.6	[80Tsa]
8.0	9.548	359.6	[80Tsa]
9.0	9.337	354.6	[80Tsa]
10.0	9.198	349.5	[80Tsa]
11	9.317	360.0	[68Bet]
12.0	8.906	349.9	[80Tsa]
15.0	8.562	351.2	[80Tsa]
17.5	8.216	348.6	[80Tsa]
20.0	7.905	353.0	[80Tsa]
20	7.4	330	[66Jen]
25.0	7.317	343.6	[80Tsa]
26.5	7.163	344.8	[80Tsa]
28.0	7.018	346.5	[80Tsa]
28	6.899	356.5	[68Bet]
30.0	6.793	344.9	[80Tsa]
34.0	6.362	343.2	[80Tsa]
49	4.870	344.1	[68Bet]
50	4.5	325	[66Jen]
69	3.025	333.4	[68Bet]
75	2.7	321	[66Jen]
80	2.651	333.1	[68Bet]
82	2.607	329.7	[68Bet]
89	2.512	310.6	[68Bet]
90	2.4	309	[66Jen]
95	2.5	311	[66Jen]

***74Wan:** R. Wang and Y.B. Kim, "Metastable Solubility Limits of Primary HCP Solid Solutions Quenched from the Liquid State," *Metall. Trans., 5,* 1973-1977 (1974). (Meta Phases; Experimental)

75Gsc: K.A. Gschneidner, Jr., "Alloys and Intermetallic Compounds," in *Scandium, Its Occurrence, Chemistry, Physics, Metallurgy, Biology and Technology,* C.T. Horovitz, Ed., Academic Press, London, 252-322 (1975). (Crys Structure; Review)

76Kub: O. Kubaschewski-von Goldbeck, "Phase Diagrams," *Zirconium: Physico-Chemical Properties of its Compounds and Alloys,* O. Kubaschewski, Ed., At. Energy Rev., Special Issue No. 6, IAEA, Vienna, 67-139 (1976). (Equi Diagram; Review)

76Wan: R. Wang, "Solubility and Stability of Liquid-Quenched Metastable h.c.p. Solid Solution," *Mater. Sci. Eng., 23,* 135-140 (1976). (Meta Phases; Experimental)

78Ved: M.V. Vedernikov, V.G. Dvunitkin, and A. Zhumagulov, "Regularities of the Behavior of Electrical Resistivity and e.m.f. in Continuous Solid Solutions of Binary Metallic Systems," *Fiz. Tverd. Tela, 20,* 3302-3305 (1978) in Russian; TR: *Sov. Phys. Solid State, 20,* 3291-3294 (1978). (Thermo; Experimental)

80Tsa: T.-W.E. Tsang, K.A. Gschneidner, Jr., and F.A. Schmidt, "Low-Temperature Heat Capacity of Sc-Zr and Sc-Mg Alloys," *Phys. Rev. B, 21,* 3100-3109 (1980). (Thermo; Experimental)

84Lop: J.M. Lopez and J.A. Alonso, "The Atomic Size-Mismatch Contribution to the Enthalpy of Formation of Concentrated Substitutional Metallic Solid Solutions," *Phys. Status Solidi (a), 85,* 423-428 (1984). (Thermo; Theory)

86Gsc: K.A. Gschneidner, Jr. and F.W. Calderwood, "Intra Rare Earth Binary Alloys: Phase Relationships, Lattice Parameters and Systematics," *Handbook on the Physics and Chemistry of Rare Earths,* Vol. 8, K.A. Gschneidner, Jr. and L. Eyring, Ed., North-Holland Physics Publishing, Amsterdam, 1-161 (1986). (Equi Diagram, Crys Structure; Compilation)

*Indicates key paper.

#Indicates presence of a phase diagram.

Sc-Zr evaluation contributed by **A. Palenzona** and **S. Cirafici,** Institute of Physical Chemistry, University of Genova, C. so Europa, Palazzo delle Scienze, 16132 Genova, Italy. This work was supported by ASM International. Literature searched through 1988. Professor Palenzona is the Alloy Phase Diagram Program Category Editor for binary rare earth alloys.

The Ag-Te (Silver-Tellurium) System

By I. Karakaya
Middle East Technical University
and
W.T. Thompson
Royal Military College of Canada

Equilibrium Diagram

The condensed phases of the Ag-Te system are: the liquid, L, with a miscibility gap; and five solid phases—fcc (Ag), hexagonal (Te), Ag_2Te, $Ag_{1.9}Te$, and Ag_5Te_3. The assessed Ag-Te phase diagram at standard atmospheric pressure is shown in Fig. 1, with experimental data points plotted in Fig. 2 and enlargements of important features shown in Fig. 3. The approximate position of the two-phase liquid-gas region is calculated form the available thermodynamic properties. A list of invariant points is given in Table 1, in which two sets of temperatures and compositions are listed for the polymorphic transformations of the nearly stoichiometric compounds Ag_2Te, $Ag_{1.9}Te$, and Ag_5Te_3. One set applies to the Ag-rich stoichiometry and the other to the Te-rich stoichiometry.

Liquidus

With the exception of the miscibility gap, the phase boundaries for the liquid field were established from cooling curves [06Pel, 10Pel, 16Chi, 39Koe]. The presence of a miscibility gap was established by [40Kra] and [66Kra]; this was confirmed, and the critical temperature of 1115 °C was reported by [69Wob] and [71Wob] from viscosity, density, and surface property measurements of molten alloys.

(Ag) and (Te)

The solid solubility of Te in (Ag) [39Koe] and that of Ag in (Te) [39Koe, 63Kuj, 65Kuj] are negligible. The distribution coefficients from segregation studies [63Kuj, 65Kuj] indicate that the

Table 1 Special Points of the Assessed Ag-Te Phase Diagram

Reaction	Compositions(a) of the respective phases, at.% Te			Temperature(b), °C	Reaction type
$L \leftrightarrow Ag$		0		961.93	Melting
$L_2 \leftrightarrow L_1 + \gamma Ag_2Te$	30.3	11.9	33.3	881	Monotectic
$L_1 \leftrightarrow (Ag) + \gamma Ag_2Te$	11.5	~0	33.3	869	Eutectic
$\gamma Ag_2Te \leftrightarrow \beta Ag_2Te$		33.3(33.8)		802 (689)	Polymorphic
$\beta Ag_2Te + L_3 \leftrightarrow \beta Ag_{1.9}Te$	33.6	51.7	34.5	460	Peritectic
$L \leftrightarrow Te$		100		449.57	Melting
$\beta Ag_{1.9}Te + L_3 \leftrightarrow \beta Ag_5Te_3$	34.7	55.6	37.8	420	Peritectic
$L_3 \leftrightarrow \beta Ag_5Te_3 + (Te)$	66.7	38.0	~100	353	Eutectic
$\alpha Ag_5Te_3 \leftrightarrow \beta Ag_5Te_3$		37.65(38.03)		265 (295)	Polymorphic
$\alpha Ag_{1.9}Te \leftrightarrow \beta Ag_{1.9}Te$		34.35(34.7)		178 (178)	Polymorphic
$\alpha Ag_2Te \leftrightarrow \beta Ag_2Te$		33.3(33.3)		145 (145)	Polymorphic
$\alpha Ag_{1.9}Te \leftrightarrow \alpha Ag_2Te + \alpha Ag_5Te_3$	34.5	33.3	37.85	120	Eutectoid

(a) Compositions in parentheses are phase boundaries with excess Te. (b) Temperatures in parentheses are for phase transformations with excess Te.